Journal of Instrumentation

TECHNICAL REPORT • OPEN ACCESS

METU-DBL: a cost effective proton irradiation facility

To cite this article: E. Karadöller *et al* 2023 *JINST* **18** T06010

Jinst

PUBLISHED BY IOP PUBLISHING FOR SISSA MEDIALAB

RECEIVED: *March 3, 2023*
REVISED: *May 24, 2023*
ACCEPTED: *June 5, 2023*
PUBLISHED: *June 26, 2023*

TECHNICAL REPORT

METU-DBL: a cost effective proton irradiation facility

E. Karadöller,[a,*] **S. Uzun Duran,**[b,a] **U. Kılıç,**[a] **R.K. Hashmani,**[a] **M.B. Demirköz,**[a] **I. Efthymiopoulos,**[c] **A.B. Can,**[a,1] **S. Çakmakoğlu,**[a,1] **B. Muçogllava,**[a,1] **A. Kayaalp**[a,1] **and C. Zorlu**[a,1]

[a] *IVMER (The Research and Application Center for Space and Accelerator Technologies), Middle East Technical University, Ankara, 06800, Türkiye*

[b] *Vocational School of Health Sciences, Program of Medical Imaging Techniques, Karadeniz Technical University, Trabzon, 61080, Türkiye*

[c] *CERN, Geneva, Switzerland*

E-mail: egecan.karadoller@metu.edu.tr

ABSTRACT: The Middle East Technical University Defocusing Beamline (METU-DBL) is designed to deliver protons with selectable kinetic energies between 15–30 MeV, and proton flux between 10^6–10^{10} protons/cm^2/s, on a maximum 21.55 to 15.40 cm target region with a beam uniformity within ±6%, in accordance with the ESA ESCC No. 25100 specification for single event effects (SEEs) tests in the low energy range. The achieved high proton fluences, allow users to test space-grade materials; electronic circuits, ASICs, FPGAs, optical lenses, structural elements, and coating layers for LEO, GEO, and interplanetary missions.

The total received dose on the Device-Under-Test (DUT) from secondary particles created during proton-material interactions at the first beam collimator and the beam dump never exceed 0.1% of the dose from primary protons. The METU-DBL is equiped with several measurement stations and services to the user teams. A secondary measurement station in a rotating drum that can hold multiple samples has been constructed next to the first collimator which provides neutrons for transmission experiments. At the target region, a robotic table is located, which provides mechanical and electrical mounting points to the samples and allows multiple samples to be tested in a row. A modular vacuum box can also be attached on the robotic table for any test that may require a vacuum environment. Power rails on the robotic table provide various outputs for the DUT. For the data acquisition, high-speed networking and a modular industrial PC are available at the target station.

[1] Formerly affiliated.
[*] Corresponding author.

https://doi.org/10.1088/1748-0221/18/06/T06010

2023 JINST 18 T06010

The design of the METU-DBL control software enables test users to integrate and optimize the data acquisition and controlling of the DUT.

The beam properties at the target region are measured with the diamond, Timepix3, and fiber scintillator detectors mounted on the robotic table. With diamond and Timepix3 detectors, measurements are taken from the five different points (center and the four corners) of the test area to measure the proton flux and ensure that it is uniform across the full test area. Fiber scintillators on both axes (X and Y) scan the target area to cross-check the beam profile's uniformity. Secondary doses during the irradiation are measured by a Geiger-Müller tube sensitive to electrons and gammas above 0.1 MeV and by a neutron detector located at the entrance of the R&D room. The room cools down relatively fast after any irradiation ($<$ 1 hour).

Accurate linear energy deposition rates and absorbed doses on the samples are calculated using MCNP6, FLUKA and Geant4 Monte Carlo simulations. Alanine dosimetry measurements that are calibrated against these simulations are also used to estimate the absorbed dose on the sample.

Keywords: Accelerator Subsystems and Technologies; Beam-line instrumentation (beam position and profile monitors, beam-intensity monitors, bunch length monitors); Hardware and accelerator control systems; Radiation damage to electronic components

2023 JINST 18 T06010

Contents

1 Introduction 1
- 1.1 Summary of space radiation environment 1
- 1.2 Summary of effects of particle radiation and radiation testing specifications 1
- 1.3 Summary of SEEs testing facility specifications according to ESA ESCC No. 25100 2

2 METU defocussing beamline 2
- 2.1 Beam uniformity measurements 3
  - 2.1.1 Scanning fiber scintillator detector 3
  - 2.1.2 Diamond detector 4
  - 2.1.3 TimePix3 detector 5
- 2.2 Instruments and systems 5
  - 2.2.1 Robotic table 5
  - 2.2.2 Neutron irradiation setup 7
- 2.3 Test procedure and reporting 7

3 Conclusion 8

1 Introduction

1.1 Summary of space radiation environment

Radiation sources in space include Van Allen Belts, Solar Particle Events and Galactic Cosmic Rays. Van Allen Belts are electrons and protons trapped in the Earth's magnetic field [1]. Solar Particle Events are electrons, protons and heavier ions ejected from the Sun. These particles reach the Earth in a couple of days and cause an increase in radiation flux for several days [2]. Galactic Cosmic Rays are charged particles accelerated near the speed of light and originating from the outside of the solar system [2].

Particles of Galactic origin consist of 85% protons, 14% alpha particles and 1% heavy ions. Particles of solar origin consist of 90–95% protons, 5–10% alpha particles and very small number of heavier ions [3]. These particles are trapped in regions in the vicinity of the Earth's geomagnetic field. The energy of particles increases as we go from solar to galactic origin. At low energies from 1 keV to 10 MeV trapped and solar protons and electrons dominate, while at high energies cosmic ray protons, alpha particles and ions dominate.

1.2 Summary of effects of particle radiation and radiation testing specifications

Radiation effects on spacecraft components can be separated into two groups: cumulative and single-event effects.

Cumulative effects lead to the progressive degradation of components' characteristics and can be separated into two sub-effects: total Ionizing Dose (TID) and displacement Damage (DD). TID effects are induced by the transfer of ionizing energy from radiation exposure. This energy is thermalized in the creation of electron-hole pairs in the material. This produces a variety of effects on the characteristics of the components such as flat band and voltage current shifts, leakage and timing skews [4]. TID tests are specified by ESA ESCC No. 22900 [5]. DD effects are induced by the non-ionizing transfer of energy. This interaction happens between primary or secondary energetic particles and component atoms. This creates damage and stable electrically active defects in crystal lattice of components [4].

The charge deposited by a single particle can produce several temporary and permanent effects. SEEs tests are specified by ESA ESCC No. 25100 [6]. The first subgroup of SEEs are non-destructive SEEs, also called soft errors. A single-event transient is a temporary voltage spike at a node in an integrated circuit and is separated into two subgroups: analog and digital. A single event upset is a single bit flip for example in flip-flops, latches or SRAM cells. A single-event functional interrupt is a soft error that causes the component to reset, lock up or malfunction. The second subgroup of SEEs are destructive SEEs that cause permanent damage. An example of a single event latch-up is the triggering of a parasitic thyristor, while a single event burnout is the triggering of a parasitic bipolar structure in a power transistor avalanche and the subsequent high current condition [4]. Details of other types of SEEs including multiple-cell upset, multiple-bit upset, single event snap-back, single event hard error, single event gate rupture and single event dielectric rupture can be found in the referenced handbook.

1.3 Summary of SEEs testing facility specifications according to ESA ESCC No. 25100

ESA ESCC No. 25100 also specifies beam parameters and testing requirements. Some parameters are given as ranges due to the test plan often being mission specific. Proton beam energy shall be in the energy range 20–200 MeV. Available exposure area should be large enough to irradiate multiple samples at the same time or fit a main board PCB. The area of 15.40 cm to 21.55 cm is given as an example of a typical board used in SEE facilities. This area can be smaller depending on the application. Proton flux shall be between 10^5 to at least 10^8 p/cm^2/s. Proton fluence shall be at least 10^{11} p/cm^2. Finally, beam homogeneity which is defined as radiation uniformity over the area of the device under test, in terms of both fluence and energy shall be uniform to $\pm 10\%$ [6].

2 METU defocussing beamline

The METU-DBL, shown in figure 1, project was started in 2015 and completed in 2021 [7]. A continuous proton beam between 15–30 MeV is delivered by TENMAK PAF [8] to METU-DBL, where the beam is collimated and then expanded to a maximum 15.40×21.55 cm area by 3 quadrupole magnets and a long flight path. The exposure area can be adjusted to smaller sizes by adjusting quadrupole magnets. The measured Beam parameters shown in table 1 confirm that the METU-DBL is able to perform tests according to ESA ESCC No. 25100 specification in the low energy range.

In addition, TID tests can be performed on the same campus by using a Co-60 source according to ESA ESCC No 22900 specification [9]. Users can test for SEE and TID back to back and compare results if needed. Also, the wide range of experimental support equipment offered such as a vacuum

2023 JINST 18 T06010

Table 1. The METU-DBL beam parameters.

Proton Energy	15–30 MeV
Exposure Area	max. 15.40×21.55 cm
Proton Flux	$10^5 - 10^{10}$ p/cm^2/s
Homogeneity	$\pm$ 6 %
Fluence	$\gtrapprox 10^{11}$ p/cm^2

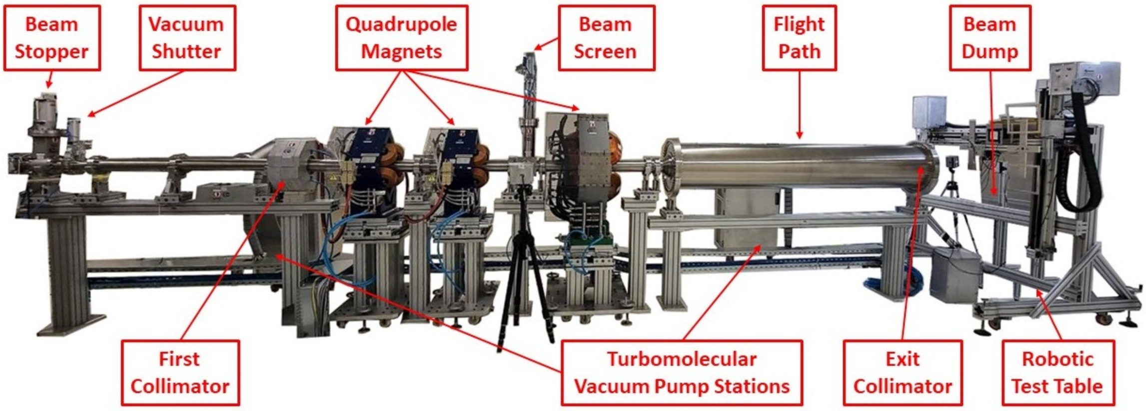

Figure 1. The METU-DBL test setup.

box, several mechanical and electrical supply connections and data acquisition options enable users to perform their test in the most convenient way.

2.1 Beam uniformity measurements

Beam uniformity measurements are performed before each irradiation session to ensure a high-quality test that conforms to the specification. Each session starts with beam parameter adjustments in cooperation with TENMAK PAF. When the beam reaches the target area, it is scanned in both horizontal and vertical directions with long fiber scintillator detectors, which measure the homogeneity of the beam. If the beam is not homogeneous enough, its parameters can be re-adjusted and the measurements repeated. The proton flux is measured at the 4 corners and the center of the target area with a diamond detector. This measurement also verifies the homogeneity measurement. If the proton flux is not homogeneous or at the desired level, beam parameters are re-adjusted and the measurements repeated. As a final step, if the desired proton flux is below 10^8 p/cm^2/s, the flux is again measured from the center of the beam area with a Timepix3 detector to verify the previous flux measurement. Irradiation starts only if measurements are in line with the requirements of the test. The beam flux and homogeneity are measured also at the end of the test to monitor possible degradation in the testing conditions during the testing period.

2.1.1 Scanning fiber scintillator detector

Fiber scintillator electronics are designed by METU-IVMER. It is a radiation hard scintillation counter, shown in figure 2, which contain 4 plastic scintillating fibers readout by a 4-channel PIN diode that is designed and manufactured by the TÜBİTAK BİLGEM UEKAE YİTAL semiconductor

2023 JINST 18 T06010

Figure 2. Scanning fiber scintillator detector.

fabrication laboratory. Scintillators were manufactured by Saint-Gobain Crystals and are fiber type BCF-60 with color green emission peaks at 530 nm. They scintillate about 7100 photons per MeV and have a decay time of 7 ns. Each of the 4 scintillators have an active area of 0.3×24 cm. Four long fibers which are stacked sideways, face the beam and scan the target area in steps of 1.2 cm with the help of a robotic table. The detector read out resolution is 12-bit. The data transfer and detector gain control are done over ethernet protocol. Adjustable gain functionality allows the detector to measure flux range between $10^5 - 10^{10}$ p/cm^2/s. The scintillator Detector is used for beam homogeneity measurements along vertical and horizontal directions. The beam homogeneity is determined by scanning the beam and acquiring the integrated flux along both the horizontal and the vertical directions separately in the target area with a maximum of $\pm 10\%$ error using the fiber scintillators. PIN diodes are covered with a light-tight housing to prevent excess reading from light leakage. Fibers covered with thin reflective aluminum tape to increase light collection efficiency and electric tape to make them light-tight.

2.1.2 Diamond detector

Figure 3. Diamond detector.

The B1 sCVD Diamond Detector, shown in figure 3 is designed and produced by Cividec Instrumentation [10]. It is read out by an ADC and a data capture board. Data is transferred to an industrial

2023 JINST 18 T06010

PC in the irradiation room over USB protocol. The sensor has an area of 4.5×4.5 mm^2 and a thickness of 500 µm. It can read proton fluxes up to 10^8 p/cm^2/s and is used for the proton beam flux measurements. The proton flux is determined from 5 points: the 4 corners and the center of the target area.

2.1.3 TimePix3 detector

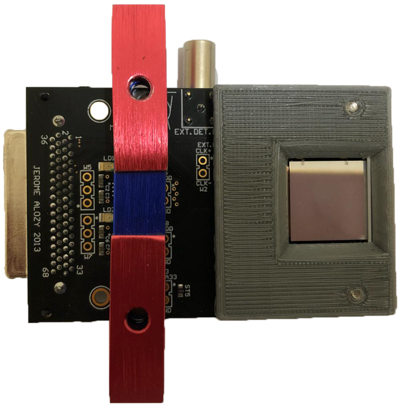

Figure 4. The Timepix3 chip and AdvaDAQ read out card with its heatsinks.

The Timepix3 chip is designed by CERN and the Medipix Collaboration [11]. The chip read out circuit is designed by Advacam [12]. The detector without its shield is shown in figure 4. It consists of 256×256 pixels with a spatial resolution of 55 µm, a time resolution of 1.5 ns, and a maximum read out of 40 million pixels/s. It is used for proton flux measurements and can measure proton fluxes up to 10^7 p/cm^2/s. The proton beam flux is measured from the target area's center if desired flux is less than 10^8 p/cm^2/s to cross-check the Diamond detector flux measurement.

2.2 Instruments and systems

A general-purpose testing facility the METU-DBL is equipped with several subsystems to meet the user requirements: a robotic target table, a vacuum box which has dimensions $35 \times 18 \times 18$ cm^3 and vacuum limit down to 10^{-3} torr, a 5 kW cooling capacity dedicated to the device under test, a neutron irradiation setup, several power supplies, data acquisition, and finally conversion and transfer systems. All electronics and radiation sensitive instrument is either located in a shield system rack or has dedicated shields designed. Any measurement equipment provided by the user can be adapted to the system due to the easy expandability of METU-DBL's infrastructure.

All systems and equipment are controlled by a color-coded slow control module shown in figure 5, developed in house in Labview. All test setups are remotely controlled from the control software that is designed specifically for each application.

2.2.1 Robotic table

The robotic table placed in the target region, shown in figure 6, allows detectors and DUT to move along horizontal and vertical axes. The table is controlled by fully automated software. It can support up to 50 kgs of weight and can move 120 cm and 80 cm in the horizontal and vertical directions respectively with a spatial accuracy of 1 mm. This instrument allows for the testing of multiple

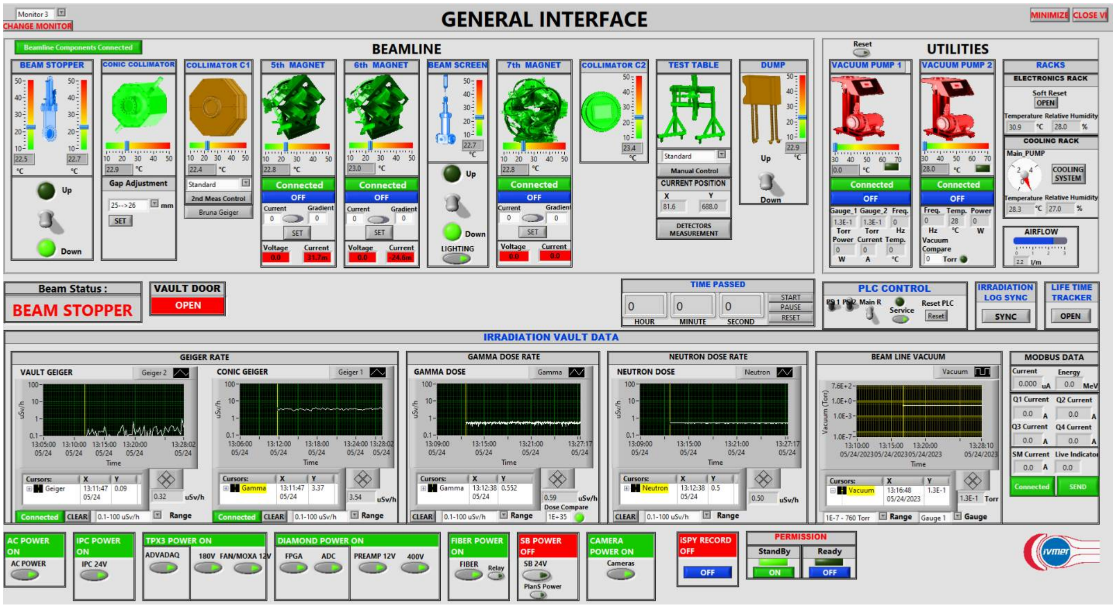

Figure 5. Slow control software.

Figure 6. The robotic table at the target region shows several movable test stations.

samples in a single irradiation session. As the robotic table moves to scan the beam or irradiate samples, there is a risk of power and data cables crossing the beam. To avoid damage from such a scenario, data and power cable channels are built into the structure of the table. A water cooled beam dump is placed behind the table to stop the beam and secondary particles. The origin of the table is considered to be the center of the exit collimator. Position calibration of the table is adjusted in the control software before every irradiation session with a positioning laser.

2.2.2 Neutron irradiation setup

Attached to the proton beamline at a 90-degree angle, centered around the collimator, there is a secondary testing station shown in figure 7. The station is built to provide a 10 cm wide neutron beam with an output neutron rate of 10^6 neutrons/cm^2/s and average neutron energy of 5 MeV. 10% of the primary protons are intercepted by the collimator, creating a large number of secondaries. The station comprises of three units: unit A encompasses the collimator and moderates the neutrons while significantly reducing electron, positron and gamma rays. Unit B is shaped like a funnel and constructed with a neutron absorbing mixture in order to reduce the initial 45 cm beam into a 10 cm diameter. This beam then passes through another gamma filter and into the testing area in Unit C, where a sample rotating system, a neutron detector, a $\beta\gamma$ Geiger-Müller tube and a camera are located. [13]. This station allows us to perform neutron transmission tests of shielding materials.

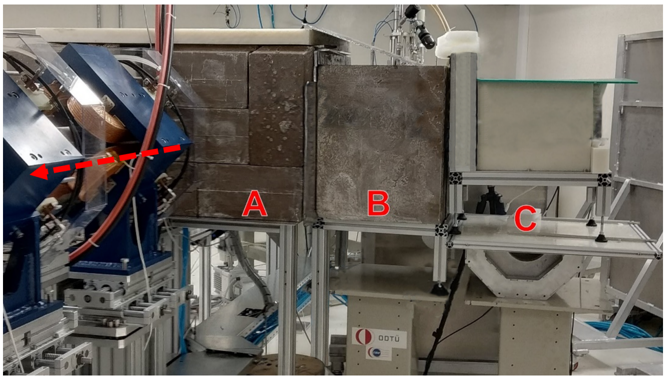

Figure 7. Neutron irradiation setup, (A) moderator, (B) neutron funnel, (C) test area.

2.3 Test procedure and reporting

The tests performed at the METU-DBL are user specific and prepared according to user requirements. The test procedure has several steps. It starts with getting information about the device or material, space orbit or trajectory, estimated mission start date and duration, and test geometry from the user. Then physics and engineering teams study the user requirements to determine the test conditions and the test preparation process starts. Monte Carlo simulations are performed by MCNP, FLUKA and Geant4 to determine irradiation time and beam parameters. Mechanical and electronic interfaces are prepared according to the test conditions, and the setup is placed in the target area. After performing the test, a final report is delivered to the user along with the returned test materials after adequate cool-down time for deactivation. The report includes target area beam parameters consisting of homogeneity, irradiation time, proton energy and flux as well as the integrated dose from gamma and neutron secondary measurements in the irradiation room. For all tests until now, the dose received from secondaries has never exceeded 1% of the dose from primary protons. In addition, the total dose received during irradiation is also measured using an alanine dosimeter which is widely used for reference dosimetry in irradiation facilities [14]. The alanine dose measurement is performed by the TENMAK NÜKEN Alanine Dosimetry Laboratory within an hour at the same campus. Upon user request data collected and additional analysis results can also be added to the final report.

2023 JINST 18 T06010

3 Conclusion

With the increasing use of miniature space crafts and space applications for satellites, the need for ground-based space radiation tests has increased. These tests are essential in minimizing the risk of failure in missions and are more cost-effective than sending a second spacecraft after failure. 18 tests have already been performed at the METU-DBL. The list of institutes includes energy, material, space, meteorology and quantum technology research centers. From the various materials tested so far, the majority consist of spacecraft electronics, coating materials and solar cells. Radiotolerant biological organisms, radiation detectors and quantum devices have been tested as well.

To summarize, the METU-DBL is a proton irradiation facility capable of SEEs tests according to ESA ESCC No. 25100 specification in the low energy range. The proton energy and flux can be adjustable between 15-30 MeV and 10^5 to 10^{10} p/cm^2/s respectively. TID tests can be performed in the same campus by using a Co-60 source in accordance with the ESA ESCC No. 22900 specification [9]. The facility has a large range of testing instrumentation and allows users to customize a suitable testing environment in a cost effective manner.

Acknowledgments

This project was supported by the Presidency of Strategy and Budget of Türkiye project number 2015K121190. M.B. Demirköz was supported by the Turkish Academy of Sciences (TÜBA), and S. Uzun Duran and B. Muçogllava were supported the Scientific and Technological Research Council of Türkiye (TÜBİTAK) 1505 project, number 5190039. The authors would like to thank TENMAK NÜKEN Proton Accelerator Facility for their support with performing radiation tests and CERN for their help in the design and validation process.

References

[1] O. Chang, *Numerical simulation of ion-cyclotron turbulence generated by artificial plasma cloud release*, Ph.D. thesis, Virginia Tech (2009).

[2] L.W. Townsend, *Space radiation environment*, in *Handbook of Bioastronautics*, Springer International Publishing (2021), pp. 335–346.

[3] G. Horneck, C. Mileikowsky, H.J. Melosh, J.W. Wilson, F.A. Cucinotta and B. Gladman, *Viable transfer of microorganisms in the solar system and beyond*, in *Astrobiology*, Springer Berlin Heidelberg (2002), pp. 57–76.

[4] ECSS, *Techniques for radiation effects mitigation in ASICs and FPGAs handbook*, Tech. Rep. ECSS-Q-HB-60-02A, ESA Requirements and Standards Division (2016).

[5] ESCC, *Total dose steady-state irradiation test method*, Tech. Rep. ESCC Basic Specification No. 22900, Space Components Ad Hoc Committee (2016).

[6] ESCC, *Single events effects test method and guidelines*, Tech. Rep. ESCC Basic Specification No. 25100, Space Components Ad Hoc Committee (2014).

[7] B. Demirköz, A. Gencer, D. Kiziloren and R. Apsimon, *Proposal for an irradiation facility at the TAEK SANAEM Proton Accelerator Facility*, *Nucl. Instrum. Meth. A* **730** (2013) 232.

2023 JINST 18 T06010

[8] A. Yuksel, G. Turemen, S. Bulut, N. Serin and O. Yavas, *Design of beam instrumentation for in-vacuum materials irradiation and testing in a 30 MeV medical cyclotron*, *Nucl. Instrum. Meth. A* **977** (2020) 164290.

[9] R. Uzel, M.B. Demirköz, A. Özyıldırım, O. Kalkan and H. Atasoy, *In-situ total ionizing dose tests of SSPA components*, in proceedings of the *6th AMICSA Proceedings*, Gothenburg, Sweden, 15–16 June 2016, pp. 180–184.

[10] T. Williams, C. N'Diaye, D. Breton, K. Cassou, K. Dupraz, P. Favier et al., *Operation of a fast diamond γ-ray detector at the HIγs facility*, *Nucl. Instrum. Meth. A* **830** (2016) 391.

[11] T. Poikela, J. Plosila, T. Westerlund, M. Campbell, M.D. Gaspari, X. Llopart et al., *Timepix3: a 65k channel hybrid pixel readout chip with simultaneous ToA/ToT and sparse readout*, 2014 *JINST* **9** C05013.

[12] D. Turecek, J. Jakubek and P. Soukup, *USB 3.0 readout and time-walk correction method for Timepix3 detector*, 2016 *JINST* **11** C12065.

[13] B. Muçogllava, *A novel layered boron-based neutron shield design and results from neutron and gamma irradiation studies*, MSc thesis, METU (2022).

[14] M.F. Desrosiers, *Alanine-EPR high-dose radiation metrology*, in *Applications of EPR in Radiation Research*, Springer International Publishing (2014), pp. 489–507.